

## Studies of the Minimum Hydrophobicity of $\alpha$ -Helical Peptides Required To Maintain a Stable Transmembrane Association with Phospholipid Bilayer Membranes<sup>†</sup>

R. N. A. H. Lewis,<sup>‡</sup> F. Liu,<sup>‡</sup> R. Krivanek,<sup>§</sup> P. Rybar,<sup>§</sup> T. Hianik,<sup>§</sup> C. R. Flach,<sup>||</sup> R. Mendelsohn,<sup>||</sup> Y. Chen,<sup>⊥</sup> C. T. Mant,<sup>⊥</sup> R. S. Hodges,<sup>⊥</sup> and R. N. McElhane<sup>\*,‡</sup>

Department of Biochemistry, University of Alberta, Edmonton, Alberta, Canada T6G 2H7, Department of Nuclear Physics and Biophysics, Comenius University, Mlynska dolina, 842 48 Bratislava, Slovakia, Department of Chemistry, Rutgers University, Newark, New Jersey 01102, and Department of Biochemistry and Molecular Genetics, University of Colorado at Denver and Health Sciences Center at Fitzsimons, Aurora, Colorado 80045

Received September 11, 2006; Revised Manuscript Received November 15, 2006

**ABSTRACT:** The effects of the hydrophobicity and the distribution of hydrophobic residues on the surfaces of some designed  $\alpha$ -helical transmembrane peptides (acetyl-K<sub>2</sub>-L<sub>m</sub>-A<sub>n</sub>-K<sub>2</sub>-amide, where  $m + n = 24$ ) on their solution behavior and interactions with phospholipids were examined. We find that although these peptides exhibit strong  $\alpha$ -helix forming propensities in water, membrane-mimetic media, and lipid model membranes, the stability of the helices decreases as the Leu content decreases. Also, their binding to reversed phase high-performance liquid chromatography columns is largely determined by their hydrophobicity and generally decreases with decreases in the Leu/Ala ratio. However, the retention of these peptides by such columns is also affected by the distribution of hydrophobic residues on their helical surfaces, being further enhanced when peptide helical hydrophobic moments are increased by clustering hydrophobic residues on one side of the helix. This clustering of hydrophobic residues also increases peptide propensity for self-aggregation in aqueous media and enhances partitioning of the peptide into lipid bilayer membranes. We also find that the peptides LA<sub>3</sub>LA<sub>2</sub> [acetyl-K<sub>2</sub>-(LAAALAA)<sub>3</sub>LAA-K<sub>2</sub>-amide] and particularly LA<sub>6</sub> [acetyl-K<sub>2</sub>-(LAAAAAA)<sub>3</sub>LAA-K<sub>2</sub>-amide] associate less strongly with and perturb the thermotropic phase behavior of phosphatidylcholine bilayers much less than peptides with higher L/A ratios. These results are consistent with free energies calculated for the partitioning of these peptides between water and phospholipid bilayers, which suggest that LA<sub>3</sub>LA<sub>2</sub> has an equal tendency to partition into water and into the hydrophobic core of phospholipid model membranes, whereas LA<sub>6</sub> should strongly prefer the aqueous phase. We conclude that for  $\alpha$ -helical peptides of this type, Leu/Ala ratios of greater than 7/17 are required for stable transmembrane associations with phospholipid bilayers.

The synthetic peptide acetyl-K<sub>2</sub>-G-L<sub>24</sub>-K<sub>2</sub>-A-amide (P<sub>24</sub>)<sup>1</sup> and its analogues have been successfully utilized as models of the hydrophobic transmembrane  $\alpha$ -helical segments of integral membrane proteins by ourselves and others (for reviews, see refs 1 and 2). These peptides contain a long sequence of hydrophobic leucine residues capped at both the N- and C-termini with two positively charged, relatively polar lysine residues. Moreover, the normally positively charged N-terminus and the negatively charged C-terminus are blocked to provide a symmetric tetracationic peptide that will

more closely mimic the transbilayer region of natural membrane proteins. The central poly-leucine region of these peptides was designed to form a maximally stable  $\alpha$ -helix, particularly in the hydrophobic environment of the lipid bilayer core, while the dilysine caps were designed to anchor the ends of these peptides to the polar surface of the lipid bilayer and to inhibit the lateral aggregation of these peptides. In fact, CD (3, 4) and FTIR (4–6) spectroscopic studies of P<sub>24</sub> have shown that it adopts a very stable  $\alpha$ -helical conformation both in solution and in lipid bilayers, and X-ray

<sup>†</sup> Supported by a Discovery Grant from the Natural Sciences and Engineering Research Council of Canada (R.N.M.), major equipment grants from the Alberta Heritage Foundation for Medical Research (R.N.M.), a NATO Collaborative Research Grant (R.N.M. and T.H.), NIH Grant R0161855 (R.S.H.), and the John Stewart Chair in Peptide Chemistry (R.S.H.).

\* To whom correspondence should be addressed. Telephone: (780) 492-2413. Fax: (780) 492-0095. E-mail: rmcclhan@ualberta.ca.

<sup>‡</sup> University of Alberta.

<sup>§</sup> Comenius University.

<sup>||</sup> Rutgers University.

<sup>⊥</sup> University of Colorado at Denver and Health Sciences Center at Fitzsimons.

<sup>1</sup> Abbreviations: P<sub>24</sub>, acetyl-K<sub>2</sub>-G-L<sub>24</sub>-K<sub>2</sub>-A-amide; L<sub>24</sub>, acetyl-K<sub>2</sub>-L<sub>24</sub>-K<sub>2</sub>-amide; (LA)<sub>12</sub>, acetyl-K<sub>2</sub>-(LA)<sub>12</sub>-K<sub>2</sub>-amide; A<sub>24</sub>, acetyl-K<sub>2</sub>-A<sub>24</sub>-K<sub>2</sub>-amide; A<sub>12</sub>, acetyl-K<sub>2</sub>-A<sub>12</sub>-K<sub>2</sub>-amide; LA<sub>3</sub>LA<sub>2</sub>, acetyl-K<sub>2</sub>-(LAAALAA)<sub>3</sub>LAA-K<sub>2</sub>-amide; LA<sub>6</sub>, acetyl-K<sub>2</sub>-(LAAAAAA)<sub>3</sub>LAA-K<sub>2</sub>-amide; (ALA)<sub>8</sub>, acetyl-K<sub>2</sub>-(ALA)<sub>8</sub>-K<sub>2</sub>-amide; A<sub>7</sub>L<sub>10</sub>A<sub>7</sub>, acetyl-K<sub>2</sub>-A<sub>7</sub>-L<sub>10</sub>-A<sub>7</sub>-K<sub>2</sub>-amide; L<sub>3</sub>A<sub>4</sub>, acetyl-K<sub>2</sub>-A<sub>2</sub>-(LLLAAAA)<sub>3</sub>-L-K<sub>2</sub>-amide; LA<sub>2</sub>-L<sub>2</sub>A<sub>2</sub>, acetyl-K<sub>2</sub>-(LAALLAA)<sub>3</sub>-LAA-K<sub>2</sub>-amide; PC, phosphatidylcholine; PE, phosphatidylethanolamine; PG, phosphatidylglycerol; DX PC, phosphatidylcholines containing tridecanoyl (T), myristoyl (M), pentadecanoyl (PD), palmitoyl (P), and oleoyl (O) hydrocarbon chains; RP-HPLC, reversed phase high-performance liquid chromatography; CD, circular dichroism; FTIR, Fourier transform infrared; ATR-FTIR, attenuated total reflection Fourier transform infrared; DSC, differential scanning calorimetry.

diffraction (7), fluorescence quenching (8), and FTIR spectroscopic (4–6) studies have confirmed that  $P_{24}$  assumes a transbilayer orientation with the N- and C-termini exposed to the aqueous environment and the hydrophobic polyleucine core embedded in the hydrocarbon core of the lipid bilayer. DSC (3, 9–11) and  $^2\text{H}$  NMR spectroscopy (9, 10) studies have shown that  $P_{24}$  broadens the gel–liquid-crystalline phase transition of the host phospholipid bilayer and reduces its enthalpy. However,  $P_{24}$  incorporation has rather different effects on the thermotropic phase behavior and organization of zwitterionic PC (5) and PE (11) and of anionic PG (unpublished observations) bilayers, indicating that  $P_{24}$ –phospholipid interactions are dependent on the structure, charge, and hydrogen bonding capabilities of the phospholipid polar headgroups of the host model membrane. Small distortions of the  $\alpha$ -helical conformation of  $P_{24}$  are observed by FTIR spectroscopy in response to peptide–lipid hydrophobic mismatch (5).  $^2\text{H}$  NMR (12) and ESR (13) spectroscopic studies have shown that the rotational diffusion of  $P_{24}$  about its long axis perpendicular to the membrane plane is rapid in the fluid phase of the bilayer and that  $P_{24}$  exists at least primarily as monomers in the liquid-crystalline phase of POPC bilayers, even at relatively high peptide concentrations.

We have varied the structure of the two lysine-capping residues on the ends of the polyleucine helix and have replaced a residue at each end of the polyleucine sequence with a Trp residue to investigate the roles of the cationic Lys and aromatic Trp residues on the interactions of  $P_{24}$  analogues with various phospholipid bilayer model membranes (14–16). These results indicate that Lys snorkeling plays a significant role in peptide–phospholipid bilayer interactions and that the presence of adjacent Trp residues may modulate the electrostatic and hydrogen bonding interactions between the Lys residues and the phospholipid polar headgroups. We have also shown that these three peptides induce an inverted cubic phase in di-trans-unsaturated PE bilayers and that their potency at doing so is independent of their structure or of the length of the peptide polyleucine core and of the hydrophobic thickness of the host PE bilayer (17).

We have also studied the effect of varying the amino acid composition of the hydrophobic core of  $L_{24}$  by replacing half or all of the Leu residues with Ala residues. Since Leu and Ala residues both have high  $\alpha$ -helix forming propensities, particularly in a hydrophobic environment, the major effect of these Leu for Ala replacements should be to decrease the hydrophobicity of the nonpolar core of the  $L_{24}$  helix (see the Discussion). Indeed, the peptide  $(\text{LA})_{12}$  exhibits the characteristic strongly  $\alpha$ -helical conformation of  $L_{24}$  in both water, organic solvents, and membrane-mimetic systems (18) and, like  $L_{24}$ , is nearly quantitatively retained in the host phospholipid bilayer in the typical transmembrane orientation (19). However,  $(\text{LA})_{12}$  perturbs the thermotropic phase behavior of PC (19, 20) and PE (21) bilayers to a greater extent than does  $L_{24}$  at comparable peptide concentrations, as indicated by a greater decrease in the temperature and enthalpy of their gel–liquid-crystalline phase transitions and by their greater disorganization of gel-state bilayers, possibly due to its rougher surface topology.  $^2\text{H}$  NMR studies also indicate that  $(\text{LA})_{12}$  is not as potent in ordering the hydrocarbon chains of DPPC and POPC bilayers in the

liquid-crystalline phase (20). The hydrophobic mismatch-dependent shift in the gel–liquid-crystalline phase transition temperature of PC bilayers is reduced by  $(\text{LA})_{12}$  as compared to  $L_{24}$ , perhaps due to the greater conformational plasticity of  $(\text{LA})_{12}$ . Like  $L_{24}$ ,  $(\text{LA})_{12}$  also exists primarily as a monomer in liquid-crystalline POPC bilayers and, according to ESR results, orders the hydrocarbon chains and slows their motion to a greater extent than  $L_{24}$  (21, 22). Moreover, deprotonation of one of the two Lys residues at each end of the  $(\text{LA})_{12}$  molecule with an increase in pH markedly reduces the characteristic effects of this peptide on the thermotropic phase behavior and organization of the host liquid-crystalline DMPC bilayer, possibly due to some degree of peptide aggregation or a reduction in the magnitude of the electrostatic and hydrogen bonding interactions between the protonated Lys residues and the phosphate moiety of the phospholipid polar headgroup (22). In contrast, although  $A_{24}$  also exists predominantly in an  $\alpha$ -helical transmembrane orientation when reconstituted with phospholipids in the absence of water, the addition of water to these preformed bilayers results in partitioning of  $A_{24}$  primarily into the aqueous phase, where it exists in a dynamic mixture of helical and nonhelical conformers (23). Thus,  $A_{24}$  appears to have sufficient  $\alpha$ -helical propensity, but insufficient hydrophobicity, to maintain a stable transmembrane association with phospholipid bilayers in the presence of water.

To determine the minimum hydrophobicity of  $\alpha$ -helical peptides of the general structure  $A_c\text{-K}_2\text{-L}_m\text{-A}_n\text{-K}_2\text{-amide}$  (where  $m + n = 24$ ) required to form stable transmembrane associations with phospholipid bilayers, we have synthesized a number of such peptides with variations in both the relative content of Leu and Ala residues in the nonpolar core and the disposition of these residues on the helical surface. We then selected two of these peptides,  $\text{LA}_3\text{LA}_2$  and  $\text{LA}_6$ , the hydrophobicities of which are near the threshold required for a stable transmembrane association with lipid bilayers, and characterized their conformational stability in water, organic solvents, and SDS micelles and their propensity to aggregate in aqueous solution. We have also investigated the stability of the interactions of these two peptides with PC bilayer model membranes of varying hydrophobic thicknesses.

## MATERIALS AND METHODS

The phospholipids used in this study (>99% pure) were obtained from Avanti Polar Lipids Inc. (Alabaster, AL) and were used without further purification. Commercially supplied solvents of at least analytical grade quality were redistilled prior to use. Peptides were synthesized and purified as trifluoroacetate salts using previously published solid phase synthesis and RP-HPLC procedures (18).

CD spectra were recorded at 20 °C on a Jasco J-500C spectropolarimeter (Jasco, Easton, MD) interfaced with a computer via a Jasco IF500II interface. The instrument was routinely calibrated with an aqueous solution of recrystallized  $d_{10}\text{-}(+)\text{-camphorsulfonic acid}$ . The data were collected at 0.1 nm resolution with a scan speed of 50 nm/min from 250 to 190 nm. Peptide concentrations ( $\sim 1.5$  mg/mL) were determined by amino acid analysis. Interpretation of the CD spectra in terms of secondary structure content was achieved by the methodology developed by Baldwin and co-workers (24).

Isothermal and temperature profiling reversed phase HPLC analyses of these peptides were performed with an Agilent 1100 series liquid chromatograph (Agilent Technologies, Little Falls, DE), equipped with a Zorbax 300 SB-C<sub>8</sub> column [150 mm × 2.1 mm (inside diameter), 5 μm particle size, 300 Å pore size]. The isothermal studies were performed using a linear AB gradient where eluent A consists of 0.05% aqueous TFA and eluent B consists of 0.05% TFA in *n*-propanol. The gradient was started with a 95/5 A/B mixture which increased linearly with time to eluent B over a period of 85 min at a flow rate of 0.25 mL/min. The temperature profiling analyses were performed using a linear A/B gradient (1% acetonitrile/min) and a flow rate of 0.25 mL/min, where eluent A was 0.2% aqueous TFA (pH 2) and eluent B was 0.2% TFA in acetonitrile. The experiments were performed in 3 °C increments from 5 to 80 °C. The data obtained were interpreted in terms of a self-association parameter as previously described (25–27). Specifically, the retention times of the peptides during the change of temperature from 5 to 80 °C were first normalized to 5 °C through the expression  $(t_R^T - t_R^5)$ , where  $t_R^T$  is the retention time at a specific temperature of the peptide and  $t_R^5$  is the corresponding retention time of the peptides at 5 °C. The normalized retention time data of the peptides were then further normalized to that of a reference peptide through the expression  $(t_R^T - t_R^5 \text{ for peptides}) - (t_R^T - t_R^5 \text{ for the reference})$ . The reference peptide for these studies, Ac-ELEKGGLEGEKGGKELEK-amide, does not self-associate in aqueous media (26). This comparison eliminates general temperature effects (e.g., decreased solvent viscosity, greater solute diffusivity, and enhanced mass transfer) which normally result in a linear decrease in the level of peptide retention with an increase in temperature. From plots of the final normalized retention time data against temperature, the self-association parameter of each peptide was taken as the maximal value of each curve above the zero line.

Peptide hydrophobicities and hydrophobic moments were calculated with the MPEx software package obtained from S. H. White's laboratory and hydrophobicity scales derived from the experimentally derived whole residue partitioning free energy measurements published by White and co-workers (28, 29). Unless stated otherwise, calculations were performed for only the hydrophobic cores of the peptides and were based on the assumption that the peptides were completely helical.

Samples were prepared for transmission FTIR spectroscopy by codissolving lipid and peptide in methanol at a lipid-to-peptide molar ratio of 30/1. After the solvent had been removed and the film dried (see above), samples containing 2–3 mg of lipid were hydrated by vigorous mixing with 75 μL of a D<sub>2</sub>O-based buffer [50 mM Tris, 150 mM NaCl, and 1 mM NaN<sub>3</sub> (pD 7.4)]. The dispersion that was obtained was then squeezed between the CaF<sub>2</sub> windows of a heatable, demountable liquid cell (NSG Precision Cells, Farmingdale, NY) equipped with a 25 μm Teflon spacer. Once the cell had been mounted in the sample holder of the spectrometer, the sample temperature could be varied between 0 and 90 °C by an external, computer-controlled water bath. FTIR spectra were acquired as a function of temperature with a Digilab FTS-40 Fourier-transform spectrometer (Bio-Rad, Digilab Division, Cambridge, MA) using data acquisition parameters similar to those described by Mantsch et al. (30).

The experiment involved a sequential series of 2 °C temperature ramps with a 20 min inter-ramp delay for thermal equilibration, which was equivalent to a scanning rate of 4 °C/h.

Polarized ATR-FTIR spectra measurements were performed on lipid/peptide films prepared by drying methanolic solutions of the lipid/peptide (30/1) mixture onto the surface of a zinc selenide ATR crystal (angle of incidence = 45 °C). The latter was mounted on a trough plate of a horizontal ATR accessory (Spectra-Tech, Shelton, CT). Spectra were acquired at room temperature with a Mattson RS1 spectrometer equipped with a broadband MCT detector. A wire grid polarizer (Optometrics, Ayer, MA) mounted in a rotation stage was positioned in the IR beam path before the detector such that rotation of the polarizer could be accomplished without breaking the continuous dry air purge. Background and sample spectra were acquired with both s- and p-polarized radiation. Data acquisition involved the co-addition of 1024 scans at a resolution of 4 cm<sup>-1</sup> with one level of zero filling (23). Both transmission and ATR spectra were processed with software obtained from the instrument manufacturers and from the National Research Council of Canada and were plotted with Origin (OriginLab Corp., Northampton, MA).

Samples were prepared for DSC as follows. Lipid and peptide were codissolved in methanol to attain the desired lipid-to-peptide ratio, and the solvent was removed with a stream of nitrogen, leaving a thin film on the sides of a clean glass test tube. This film was subsequently dried in vacuo overnight to ensure removal of the last traces of solvent. Samples containing 0.5–0.8 mg of lipid were then hydrated by vigorous vortexing with a buffer [50 mM Tris, 150 mM NaCl, and 1 mM NaN<sub>3</sub> (pH 7.4)] at temperatures approximately 10–15 °C above the gel–liquid-crystalline phase transition temperature of the lipid. DSC thermograms were obtained from 0.5 mL samples with a high-sensitivity Microcal VP-DSC instrument (Microcal Inc., Northampton, MA) operating at heating and cooling rates of 10 °C/h.

## RESULTS

We have studied a number of α-helical transmembrane peptides of the general structure acetyl-K<sub>2</sub>-(L<sub>*m*</sub>+A<sub>*n*</sub>)-K<sub>2</sub>-amide, where the L/A ratio has been varied from 24/0 (L<sub>24</sub>) to 0/24 (A<sub>24</sub>), to study how variations in the hydrophobicity of the nonpolar peptide core affect their conformation, conformational stability, and self-association propensities, as well as their associations with lipid membranes. The helical net representations of the some of these peptides are shown in Figure 1. With the two peptides on which we focus here (i.e., LA<sub>6</sub> and LA<sub>3</sub>LA<sub>2</sub>), all of the Leu residues are linearly clustered along one face of the α-helix, as is also the case with the peptide LA<sub>2</sub>L<sub>2</sub>A<sub>2</sub>. Also, the Leu residues of peptides such as (LA)<sub>12</sub> and (ALA)<sub>8</sub> are spirally distributed on the surface of the α-helix, whereas with A<sub>7</sub>L<sub>10</sub>A<sub>7</sub> (not shown), they are horizontally distributed around the center of the helix. Finally, with L<sub>3</sub>A<sub>4</sub>, a compositional isomer of peptides LA<sub>2</sub>L<sub>2</sub>A<sub>2</sub> and A<sub>7</sub>L<sub>10</sub>A<sub>7</sub>, Leu residues are fairly evenly distributed on the helical surface among alternating linear strips of Leu and Ala residues (see Figure 1). The study of these α-helical peptides should thus provide valuable insight into how the capacity to form stable transmembrane associa-



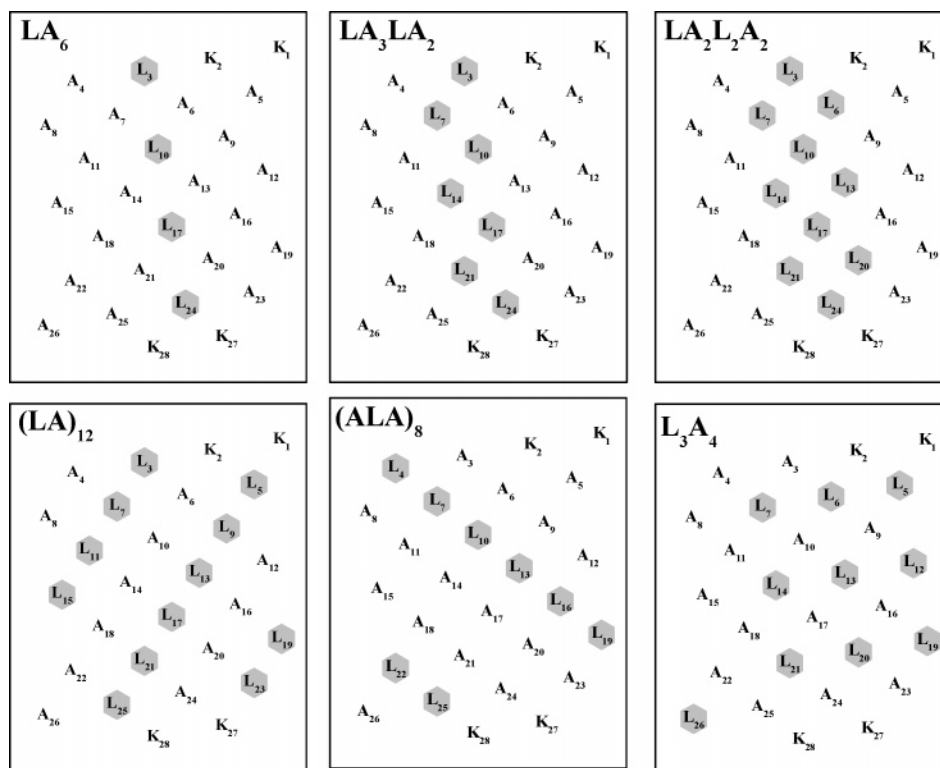


FIGURE 1: Helical net representations of selected members of the acetyl-K<sub>2</sub>-(L<sub>m</sub>-A<sub>m</sub>)-K<sub>2</sub>-amide family of model transmembrane  $\alpha$ -helical peptides that were studied. The leucine residues forming the hydrophobic surfaces of the peptides are highlighted.

tions with phospholipid bilayers can be affected by both the amino acid composition and the spatial distribution of amino acid side chains on their surfaces.

To experimentally determine the effective hydrophobicities of this series of peptides, their retention times on a RP-HPLC column were determined. These analyses were performed at 70 °C to minimize effects that can be attributed to self-association in the aqueous phase (see below), and the retention times that were measured are plotted against the calculated values for the overall hydrophobicities of these peptides (Figure 2A). As expected, the RP-HPLC retention times generally increase as the L/A ratio and thus the hydrophobicity increases, indicating that overall peptide hydrophobicity is the dominant factor in the retention of these peptides by the hydrophobic stationary phase of the RP-HPLC column. However, there is also considerable scatter of the data points about the regression line, suggesting that the RP-HPLC retention times are also influenced by the distribution of the Leu and Ala residues on the helical surfaces of these peptides. This is illustrated by the observation that the retention times of A<sub>7</sub>L<sub>10</sub>A<sub>7</sub>, L<sub>3</sub>A<sub>4</sub>, and LA<sub>2</sub>L<sub>2</sub>A<sub>2</sub> (compositionally isomeric peptides with Leu/Ala ratios of 10/14) increase in the following order, despite the fact that their overall hydrophobicities are nominally the same: A<sub>7</sub>L<sub>10</sub>A<sub>7</sub> < L<sub>3</sub>A<sub>4</sub> < LA<sub>2</sub>L<sub>2</sub>A<sub>2</sub>. This aspect of the RP-HPLC retention behavior of this family of model transmembrane peptides was explored by correlating the retention times with the hydrophobic moments of the  $\alpha$ -helical structures formed (see below).

A plot of the RP-HPLC retention times of these model transmembrane peptides against their helical hydrophobic moments (Figure 2B) suggests that they can be broadly separated into three groups, as indicated by the connecting lines that are drawn. The group exemplified by peptides A<sub>24</sub>,

A<sub>7</sub>L<sub>10</sub>A<sub>7</sub>, (LA)<sub>12</sub>, and L<sub>24</sub> (connected by the solid line) have low helical hydrophobic moments (i.e., they form weakly amphipathic  $\alpha$ -helices), because their Leu and Ala residues are essentially symmetrically distributed around the helical axis. For this group, their RP-HPLC retention times are determined essentially exclusively by their nominal hydrophobicity, as determined, in turn, by their amino acid compositions. In contrast, the group exemplified by peptides LA<sub>6</sub>, LA<sub>3</sub>LA<sub>2</sub>, and LA<sub>2</sub>L<sub>2</sub>A<sub>2</sub> (connected by the dashed line) have their Leu residues linearly clustered on one side of their helical surfaces and thus form relatively strongly amphipathic helices (note the increasing magnitudes of their helical hydrophobic moments). For this group of peptides, the level of RP-HPLC retention also increases as nominal hydrophobicity increases but, because of the clustering of their Leu residues, they also tend to be more strongly retained by RP-HPLC columns than are peptides of similar amino acid composition but lower amphipathicity. Thus, for example, LA<sub>2</sub>L<sub>2</sub>A<sub>2</sub> is more strongly retained on RP-HPLC columns than are its compositional isomers A<sub>7</sub>L<sub>10</sub>A<sub>7</sub> and L<sub>3</sub>A<sub>4</sub>, despite having identical amino acid compositions (see Figure 2). Finally, for peptides similar or comparable in amino acid composition (exemplified here by those connected by the dotted line), the differences between their RP-HPLC retention behavior are largely determined by the differences in the amphipathicity of the helical structures that are formed. However, within any such group of peptides, the differences in RP-HPLC retention behavior are small relative to that attributable to the overall hydrophobicity of such peptides.

Temperature profiling RP-HPLC was performed to study aspects of the conformational stability of these peptides and, more specifically, to compare their propensities for self-association in aqueous media. As long as increases in temperature are not accompanied by the exposure of occluded

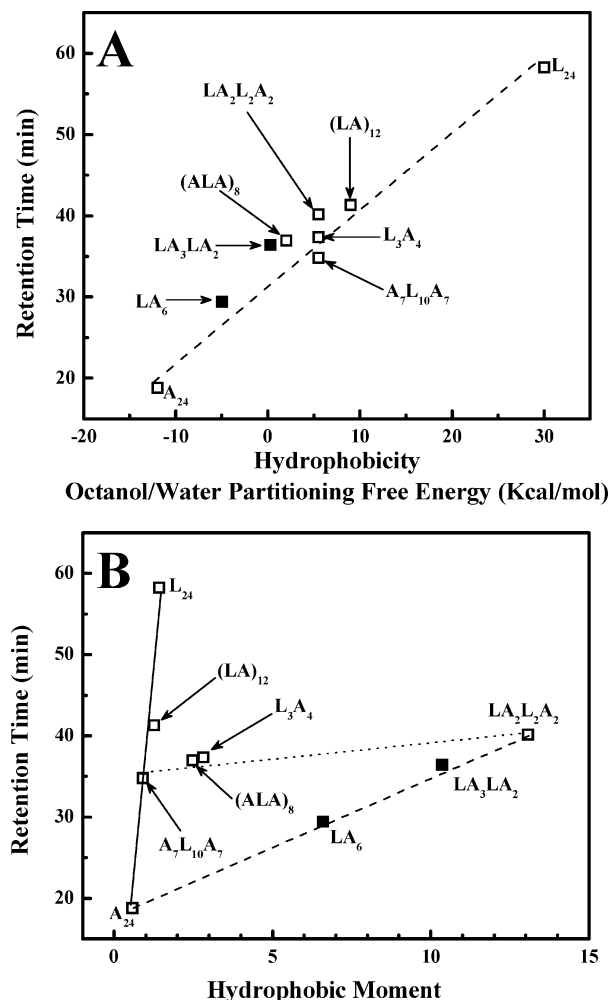


FIGURE 2: Isothermal (70 °C) RP-HPLC retention times of the acetyl-K<sub>2</sub>-(L<sub>m</sub>-A<sub>n</sub>)-K<sub>2</sub>-amide family of model transmembrane  $\alpha$ -helical peptides plotted as a function of overall peptide hydrophobicity (A) and helical hydrophobic moment (B). The data points from LA<sub>3</sub>LA<sub>2</sub> and LA<sub>6</sub>, which are the focus of this study, are highlighted by the filled symbols.

hydrophobic surfaces, peptide RP-HPLC retention times should decrease monotonically with temperature, because of the effects arising from thermally induced decreases in solvent viscosity, increases in solute diffusivity and mass transfer, etc. (25–27). However, whenever increases in temperature also increase the probability of exposing occluded hydrophobic surfaces, the thermally induced decrease in RP-HPLC retention times will be attenuated and retention times may even increase with temperature, depending on the nature of the process involved and the relative sizes of the thermally exposed hydrophobic surfaces (see refs 26 and 27). With these types of peptides, changes in the degree of self-association are essentially the only processes whereby thermally induced exposure of occluded hydrophobic surfaces can occur. Consequently, we can interpret a positive deviation of the temperature dependence of the RP-HPLC retention times of these peptides relative to that of a nonassociating reference in terms of changes in the propensity of the peptide to self-associate in aqueous media.

Illustrated in Figure 3A are the temperature dependencies of the RP-HPLC retention times of peptides LA<sub>3</sub>LA<sub>2</sub> and LA<sub>6</sub>. At all the temperatures that were examined, LA<sub>3</sub>LA<sub>2</sub> binds more strongly to the RP-HPLC column than LA<sub>6</sub>,

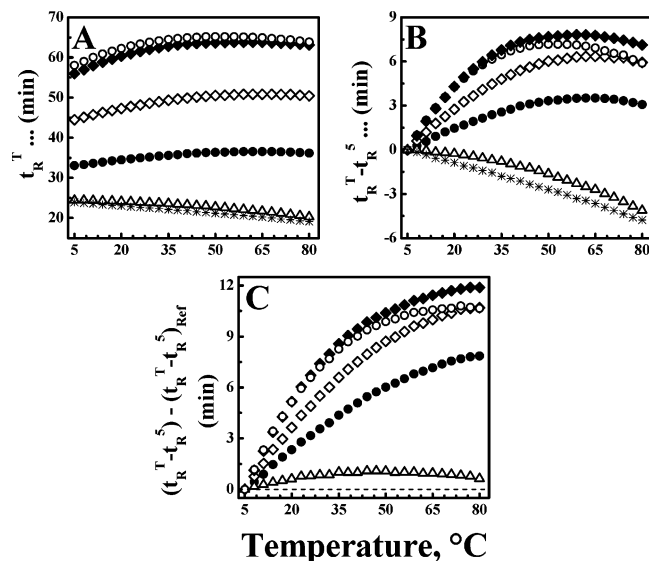


FIGURE 3: Temperature profiling HPLC studies of peptides LA<sub>3</sub>LA<sub>2</sub> (◆) and LA<sub>6</sub> (◇): (A) RP-HPLC retention times ( $t_R^T$ ), (B) temperature-corrected RP-HPLC retention times ( $t_R^T - t_R^5$ ), and (C) reference-corrected RP-HPLC retention times [ $(t_R^T - t_R^5) - (t_R^T - t_R^5)_{Ref}$ ]. For comparative purposes, data are also shown for peptides (ALA)<sub>8</sub> (○), A<sub>24</sub> (●), and A<sub>12</sub> (△) and the reference peptide, which does not self-associate in aqueous media (\*). The dashed line in panel C represents the behavior expected of the reference peptide.

consistent with its higher Leu content and greater innate hydrophobicity. Also, plots of the retention times of LA<sub>3</sub>LA<sub>2</sub> and LA<sub>6</sub> as a function of temperature describe a convex shape, with retention times increasing with temperature, reaching a plateau, and then decreasing slightly at higher temperatures (Figure 3A). This pattern of behavior differs markedly from the linear monotonic decrease exhibited in the absence of peptide self-association (see plots of the reference peptide in Figure 3A), indicating that LA<sub>3</sub>LA<sub>2</sub> and LA<sub>6</sub> are both quite prone to self-association in aqueous media. This aspect of the behavior of these peptides is more vividly demonstrated when the RP-HPLC retention times of each peptide are normalized against its retention time at 5 °C (Figure 3B) and subsequently plotted against the behavior of the reference peptide (Figure 3C). Such plots show quite clearly that the self-association propensities of this family of peptides increase markedly with peptide length (note A<sub>12</sub> < A<sub>24</sub>) and Leu content (note that A<sub>24</sub> < LA<sub>6</sub> < LA<sub>3</sub>LA<sub>2</sub>). More specifically, however, we note that the self-association propensities of this family of peptides are also influenced by the distribution of Leu and Ala residues on the helical surface. Thus, despite a higher Leu content and innate hydrophobicity, the self-association propensity of peptide (ALA)<sub>8</sub> is comparable to that of peptide LA<sub>3</sub>LA<sub>2</sub> at low temperatures but decreases to values approaching those of peptide LA<sub>6</sub> at higher temperatures (see panels B and C of Figure 3). Such behavior is probably a reflection of the fact that the Leu residues of LA<sub>3</sub>LA<sub>2</sub> and LA<sub>6</sub> are linearly clustered on one face of the helical surface, whereas those of peptide (ALA)<sub>8</sub> are spirally distributed over the entire helical surface. Thus, the observation that LA<sub>3</sub>LA<sub>2</sub> exhibits significantly higher propensities for self-association in aqueous media than LA<sub>6</sub> is the combined effect of its innately higher hydrophobicity and the fact that its Leu residues are all clustered on one face of the helical surface.

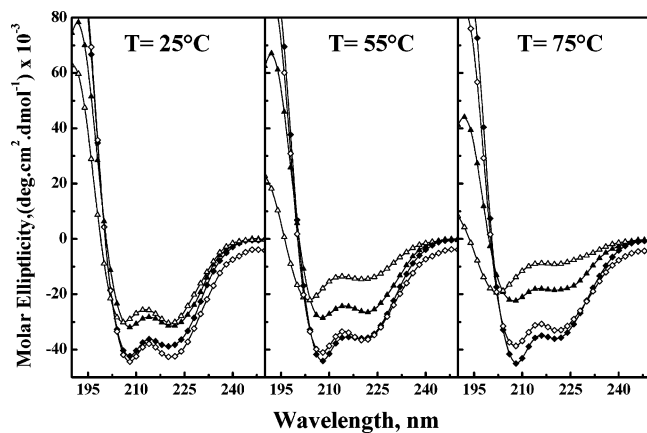


FIGURE 4: CD spectra of peptides  $LA_3LA_2$  ( $\blacklozenge$  and  $\blacktriangle$ ) and  $LA_6$  ( $\diamond$  and  $\triangle$ ). The spectra shown were acquired at the temperatures indicated with peptides dispersed in aqueous buffer ( $\blacktriangle$  and  $\triangle$ ) and in SDS micelles ( $\blacklozenge$  and  $\diamond$ ).

CD spectra of  $LA_3LA_2$  and  $LA_6$  were recorded in aqueous media and in aqueous SDS micelles at various temperatures to study the conformation and conformational stability of these peptides. At all temperatures, the CD spectra of these peptides in water and SDS micelles exhibit strong negative molar ellipticity values at  $\sim 207$ – $209$  and  $\sim 219$ – $222$  nm, indicative of a helical conformation (Figure 4). Also, the minimal molar ellipticity values of both peptides are greater in SDS micelles than in water, indicating that the greater hydrophobicity of a membrane-mimetic environment promotes helix formation, as expected and observed previously for  $L_{24}$  (4),  $(LA)_{12}$  (18), and  $A_{24}$  (23). Moreover, in both aqueous solution and SDS micelles, the maximum negative ellipticity values increase with an increase in temperature to a smaller extent in  $LA_3LA_2$  than in  $LA_6$ , indicating that the former peptide is more conformationally stable than the latter in both polar and relatively nonpolar environments. As well, the thermally induced decreases in the negative molar ellipticity values of both peptides are attenuated in SDS micelles relative to aqueous buffer, again illustrating the stabilization of helical structure in the more hydrophobic, membrane-mimetic environment.

The conformation and conformational stability of peptides  $LA_3LA_2$  and  $LA_6$  in aqueous solution and in SDS micelles were also studied by FTIR spectroscopy, and the results are summarized in Figure 5. When cast from methanol, the infrared spectra exhibited by dried films of both peptides contain strong and relatively sharp absorption bands centered near  $1658$  and  $1545$   $cm^{-1}$  arising from the amide I and amide II vibrational modes, respectively (see Figure 5A). The former arises predominantly from the stretching vibrations of the amide carbonyl groups, whereas the latter is attributed primarily to the N–H bending vibration of the amide protons (31). The frequencies of the two absorption bands also suggest that the two peptides adopt predominantly  $\alpha$ -helical conformations when cast from a methanolic solution (31). Figure 5 also shows that the properties of the amide I and amide II bands of these two peptides change significantly when dissolved in deuterated aqueous media or dispersed in micellar solutions of SDS in deuterated aqueous media. In particular, there is a substantial decrease in the intensity of the amide II band of each peptide relative to the intensity of its amide I band, indicating that considerable H–D exchange

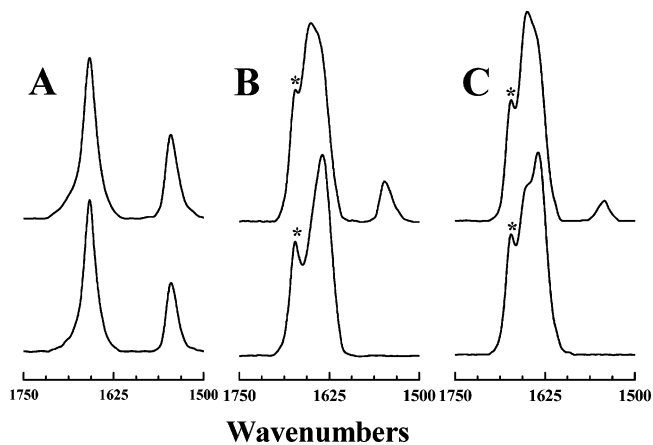


FIGURE 5: FTIR spectra exhibited by peptides  $LA_3LA_2$  (top) and  $LA_6$  (bottom) as dried films cast from methanol (A), solutions in deuterated aqueous buffer (B), and solutions in SDS micelles dispersed in deuterated aqueous buffer (C) at  $25^\circ C$ . With the hydrated samples, the marked band (\*) near  $1670$   $cm^{-1}$  arises from the trifluoroacetate counterions which copurify with the peptides.

of their amide protons has occurred. More significantly, however, the amide II band is essentially absent from the IR spectra of  $LA_6$  in both  $D_2O$  solution or SDS micelles in  $D_2O$ -based buffers, whereas under comparable conditions, significant amide I intensity persists in the IR spectra of  $LA_3LA_2$  (see Figure 5). This observation indicates that H–D exchange is much slower in  $LA_3LA_2$  than in  $LA_6$ , where nearly complete H–D exchange of the amide protons causes nearly total loss of amide II absorption at  $1546$   $cm^{-1}$  in the latter. In turn, this finding suggests that  $LA_3LA_2$  forms much more conformationally stable structures that are much more resistant to amide proton H–D exchange than does  $LA_6$ . Figure 5 also shows that the amide I band of these peptides is largely composed of two relatively strong component peaks centered near  $1650$  and  $1633$   $cm^{-1}$ . The amide I component near  $1650$   $cm^{-1}$  is indicative of  $\alpha$ -helical structure (31), whereas that near  $1633$   $cm^{-1}$  suggests the presence of a considerable amount of  $3_{10}$ -helical structure, which is often observed in Ala-rich peptides in aqueous solution (32). The amide I component centered near  $1650$   $cm^{-1}$  of both peptides is relatively stronger in SDS micelles than in aqueous media, indicating that their  $\alpha$ -helical structural propensity is greater, and their  $3_{10}$ -helical structural propensity is smaller, in a more hydrophobic, membrane-mimetic environment than in water. Also, in both media, the component near  $1650$   $cm^{-1}$  is more prominent in  $LA_3LA_2$  than in  $LA_6$ , indicating a relatively higher  $\alpha$ -helical content in the former than in the latter peptide, consistent with its higher leucine content.

FTIR spectroscopy was also used to study the conformation and conformational stability of  $LA_3LA_2$  and  $LA_6$  in phospholipid model membranes of various hydrocarbon chain lengths. The spectra illustrated in Figure 6 were recorded using  $LA_6$  incorporated in DTPC bilayers and are largely typical of the type of data that was obtained. At low temperatures, the major component of the amide I band is centered near  $1633$   $cm^{-1}$ , whereas at higher temperatures, the amide I component centered near  $1650$   $cm^{-1}$  predominates. Since this frequency shift of the amide I band occurs over the temperature interval ( $10$ – $20^\circ C$ ) encompassing the gel–liquid-crystalline phase transition temperature of DTPC, one can conclude that the majority of  $LA_6$  molecules are

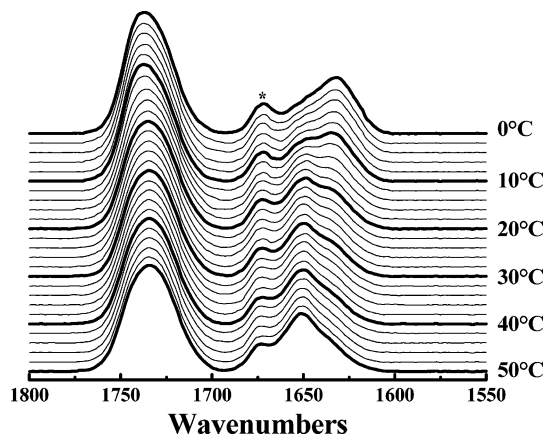


FIGURE 6: Representative FTIR spectra illustrating the type of temperature-dependent changes in the peptide amide I bands observed with mixtures of peptides LA<sub>3</sub>LA<sub>2</sub> and LA<sub>6</sub> with PC bilayers. The data set that is shown was acquired in the cooling mode using a LA<sub>6</sub> mixture with ditridecanoyl-PC bilayers at a nominal lipid/peptide ratio of 30/1. The marked component (\*) near 1670 cm<sup>-1</sup> arises from the trifluoroacetate counterions which copurify with the peptides.

incorporated into the PC bilayer, since their conformation is clearly influenced by the physical state of the host phospholipid model membrane. Moreover, since the 1633 cm<sup>-1</sup> absorption band probably arises from a 3<sub>10</sub>-helical conformation (31) and the 1650 cm<sup>-1</sup> absorption band from an  $\alpha$ -helical conformation, we conclude that LA<sub>6</sub> exists predominantly as a more extended 3<sub>10</sub>-helix in the thicker gel state and as a less extended  $\alpha$ -helix in the thinner liquid-crystalline state of the PC bilayer. Very similar results were obtained when LA<sub>3</sub>LA<sub>2</sub> was incorporated into DTPC bilayers (data not shown). A lipid phase-state-induced change in the conformation of a model transmembrane peptide was also noted in studies of peptide (LA)<sub>12</sub>, although in that case incorporation into gel-state PC bilayers of considerably greater hydrophobic thickness was required to distort the helical structure (19), probably due to the restricted conformational plasticity of (LA)<sub>12</sub> compared to LA<sub>6</sub>. However, the polyleucine-based peptides P<sub>24</sub> (4) and L<sub>24</sub> (14) form only  $\alpha$ -helices in phospholipid bilayers regardless of hydrophobic thickness.

The correlation between conformational changes in peptides LA<sub>3</sub>LA<sub>2</sub> and LA<sub>6</sub> and the gel–liquid-crystalline phase transitions of their host lipid bilayers is exemplified by the data presented in Figure 7. The FTIR spectra shown therein were acquired as function of temperature with LA<sub>3</sub>LA<sub>2</sub> incorporated into DPDPC bilayers. In the experiment that is illustrated, the CH<sub>2</sub> symmetric stretching frequency of the PC hydrocarbon chains, as well as the intensity of the amide I frequency at 1633 cm<sup>-1</sup>, was continuously monitored as the sample was heated and cooled. To facilitate a comparison of our spectroscopic and calorimetric results, the heating and cooling DSC endotherms for this system are superimposed on the spectroscopic data. In the heating mode, the gel–liquid-crystalline phase transition is clearly shown by a sudden increase in the frequency of the CH<sub>2</sub> symmetric stretching frequency from 2850.5 cm<sup>-1</sup>, which is characteristic of gel-state DPDPC bilayers, to ~2853 cm<sup>-1</sup>, which is characteristic of liquid-crystalline DPDPC bilayers (see refs 33 and 34). Note that the temperature interval over which the hydrocarbon chains undergo melting coincides closely

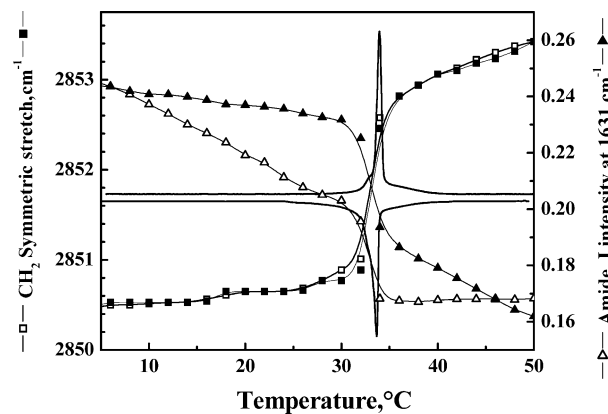


FIGURE 7: Correlation between temperature-induced changes in lipid- and peptide-derived FTIR spectroscopic markers with the gel–liquid-crystalline phase transition resolved by DSC. The data were all obtained with a 30/1 (molar ratio) mixture of dipentadecanoyl-PC with peptide LA<sub>3</sub>LA<sub>2</sub>. The solid lines indicate the DSC heating (top) and cooling (bottom) thermograms. Filled symbols depict FTIR spectroscopic data acquired in the heating mode, and empty symbols depict data obtained in the cooling mode.

with the DSC heating endotherm, as expected. Also, the proportion of LA<sub>3</sub>LA<sub>2</sub> in the extended helical conformation also decreases markedly over the temperature interval in which the PC gel–liquid-crystalline phase transition occurs, indicating that this peptide conformational change is triggered by the phospholipid chain melting phase transition. Similar results are obtained upon cooling, except that the temperature-induced peptide conformational change exhibits considerable hysteresis, whereas the conformational change in the phospholipid hydrocarbon chains does not.

Finally, we have studied the conformation of both LA<sub>3</sub>LA<sub>2</sub> and LA<sub>6</sub> in PC bilayers of various hydrophobic thicknesses at a temperature both below (0 °C) and above (50 or 66 °C) their characteristic gel–liquid-crystalline phase transition temperatures. The results of this study, presented in Figure 8, again illustrate the general shift in the amide I frequency of both peptides from ~1633 to 1650 cm<sup>-1</sup> as one goes from the phospholipid gel to liquid-crystalline state. However, the 1633 cm<sup>-1</sup> component is always less prominent, and the 1650 cm<sup>-1</sup> component of the amide I band more prominent, in LA<sub>3</sub>LA<sub>2</sub> than in LA<sub>6</sub>, when compared at the same temperature and in the same host phospholipid bilayer. This result indicates that LA<sub>3</sub>LA<sub>2</sub> has a weaker tendency than LA<sub>6</sub> to form an extended 3<sub>10</sub>-helix, as might be expected from the lower Ala content of the former. Note also that LA<sub>3</sub>LA<sub>2</sub> exhibits an amide II peak in gel-state PC bilayers and that the intensity of this peak increases as the thickness of the host PC bilayer increases. Also, LA<sub>3</sub>LA<sub>2</sub> exhibits an amide II peak in the liquid-crystalline states of the two thicker PC bilayers. In contrast, an amide II band is not observed for LA<sub>6</sub> in either the gel or liquid-crystalline phase of any PC bilayer, regardless of its hydrocarbon chain length. These observations indicate that LA<sub>3</sub>LA<sub>2</sub> is sufficiently well incorporated and well shielded from the aqueous (D<sub>2</sub>O) environment when associated with gel-state or with the thicker liquid-crystalline-state PC bilayers to be at least partially protected from H–D amide exchange, whereas this is not the case for LA<sub>6</sub>. The latter observation suggests that LA<sub>6</sub> may not be stably associated with PC bilayers in an exclusively transbilayer orientation.



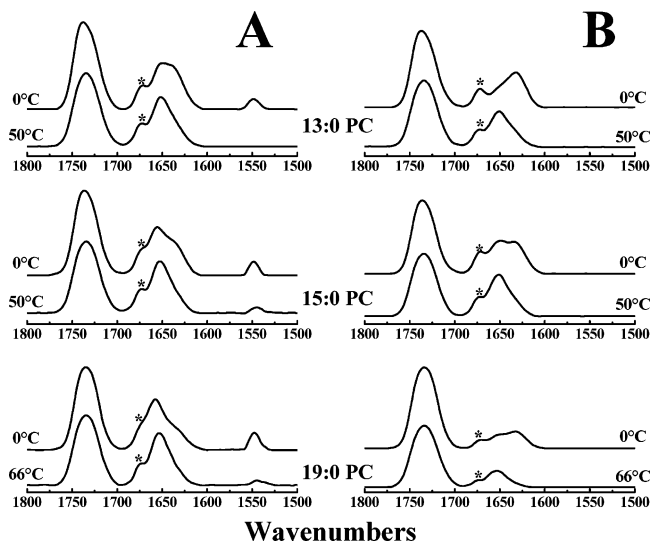


FIGURE 8: FTIR spectra of  $LA_3LA_2$ -containing (A) and  $LA_6$ -containing PC bilayers (B). The traces show the ester C=O stretching, amide I, and amide II regions of the IR spectra obtained at the temperatures and with the host lipid bilayers indicated. The spectra were all obtained using mixtures with a lipid/peptide molar ratio of 30/1. The marked component (\*) near  $1670\text{ cm}^{-1}$  arises from the trifluoroacetate counterions which copurify with the peptides.

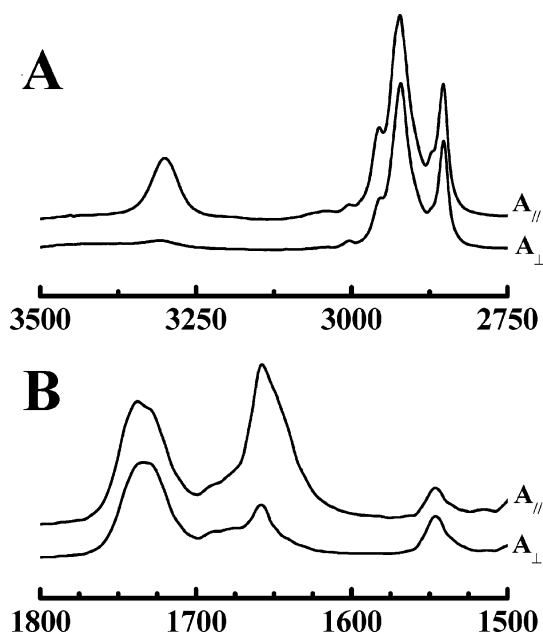


FIGURE 9: Representative attenuated total reflectance FTIR spectra of uniaxially oriented dry films of peptide-containing POPC bilayers. The C-H stretching and amide-A regions of the IR spectrum are shown in panel A, and the ester C=O stretching, amide I, and amide II regions are shown in panel B. In each panel, the top trace ( $A_{||}$ ) shows absorbance spectra acquired with p-polarized infrared radiation and the bottom trace ( $A_{\perp}$ ) shows spectra obtained with s-polarized radiation. The spectra were obtained with  $LA_6$ -containing POPC bilayers at a lipid/peptide molar ratio of 30/1.

ATR-FTIR studies were also performed to study the conformation, orientation, and degree of association of these peptides with both minimally and fully hydrated phospholipid bilayers. The data shown in Figure 9 are polarized ATR-FTIR spectra of a dry film composed of POPC and  $LA_3LA_2$  and are also typical of the results obtained in corresponding studies of  $LA_6$ . As observed with the transmission FTIR data shown earlier, these spectra also exhibit sharp amide I and

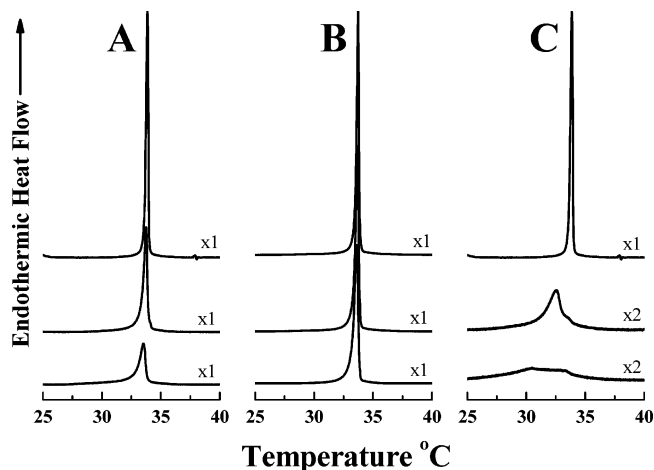


FIGURE 10: Effect of peptide concentration on the gel-liquid-crystalline phase transition of dipentadecanoyl-PC bilayers. DSC thermograms are shown for lipid/peptide mixtures containing  $LA_3LA_2$  (A),  $LA_6$  (B), and  $L_{24}$  (C). In each panel, the top trace exemplifies the DSC thermogram obtained in the absence of peptide with the middle and bottom traces representing thermograms obtained with lipid/peptide mixtures containing 3.3 and 6.7 mol % peptide, respectively. The Y-axis scaling factors are indicated beside each DSC thermogram.

amide II absorption bands centered near  $1658$  and  $1547\text{ cm}^{-1}$ , consistent with the peptide adopting a predominantly  $\alpha$ -helical conformation under these conditions. However, Figure 9 also shows that the intensity of the amide A ( $\sim 3300\text{ cm}^{-1}$ ) and amide I ( $\sim 1658\text{ cm}^{-1}$ ) bands in spectra acquired with p-polarized radiation is considerably greater ( $\sim 5$  times the integrated intensity) than that acquired with s-polarized radiation. This observation provides clear evidence that the  $LA_3LA_2$  helices are preferentially oriented in the dry film such that the amide A (N-H stretching) and amide I (C=O stretching) transition moments are aligned essentially along the normal to the surface of the ATR crystal, indicating that the long axes of the peptide helices are preferentially oriented perpendicular to the surface of the crystal. A comparable examination of the absorption bands arising from the symmetric C-H stretching vibrations of the terminal methyl groups ( $\sim 2870\text{ cm}^{-1}$ ) on the lipid hydrocarbon chains indicates that the fatty acyl chains of the lipid are also preferentially aligned perpendicular to the surface of the ATR crystal. Together, these observations provide strong evidence that  $LA_3LA_2$  is actually incorporated into the dried lipid/peptide films and that it exists in those films as a transbilayer  $\alpha$ -helix. Unfortunately, when the oriented POPC bilayers were fully hydrated by the addition of buffer, the phospholipid film floated up off the crystal surface so that their ATR-FTIR spectra could no longer be monitored. Thus, we could not determine definitively whether this peptide retained its strong association with, and its well-ordered transmembrane orientation in, fully hydrated POPC bilayers. However, the transmission FTIR data presented earlier, and the DSC data presented below, do suggest that  $LA_3LA_2$ , although perhaps not  $LA_6$ , has a moderate affinity for fully hydrated PC bilayers and is associated with those bilayers primarily as a transmembrane helix.

The effects of  $LA_3LA_2$  and  $LA_6$  on the thermotropic phase behavior of DPDP bilayers were studied by DSC, and the thermograms that were obtained are presented in Figure 10. As a control, a similar experiment was carried out with  $L_{24}$ .



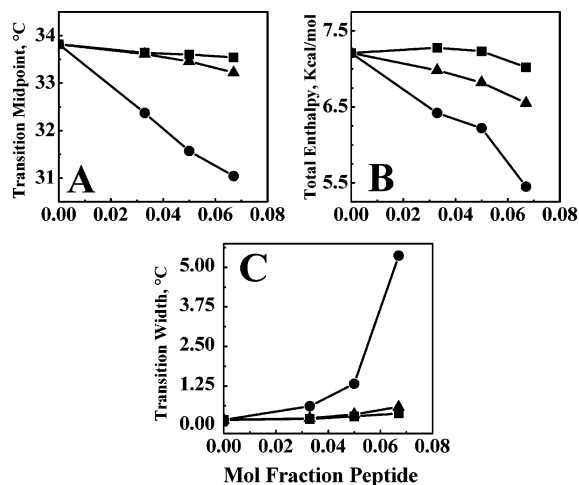


FIGURE 11: Effect of peptide concentration on the midpoint temperature (A), enthalpy (B), and width (C) of the gel-liquid-crystalline phase transition of dipentadecanoyl-PC bilayers. Data are presented for bilayers containing LA<sub>6</sub> (■), LA<sub>3</sub>LA<sub>2</sub> (▲), and L<sub>24</sub> (●).

As shown in Figure 11, the incorporation of increasing quantities of L<sub>24</sub> progressively decreased the temperature, enthalpy, and cooperativity of the gel-liquid-crystalline phase transition of DPDPC, indicating that this rather hydrophobic peptide is efficiently incorporated into the host phospholipid bilayer. In contrast, the effects of LA<sub>3</sub>LA<sub>2</sub> and particularly of LA<sub>6</sub> on the thermotropic phase behavior of DTPC were considerably attenuated such that the decreases in the temperature, enthalpy, and cooperativity of the gel-liquid-crystalline phase transition of the host phospholipid bilayer were all much smaller. Since it is unlikely that the structural differences in the nonpolar core region of these peptides would themselves have a major differential effect on perturbing the hydrocarbon chain packing in PC bilayers, it seems more likely that the increasingly attenuated effects of LA<sub>3</sub>LA<sub>2</sub> and especially of LA<sub>6</sub> on the thermotropic phase behavior of the host phospholipid bilayer are due to their increasingly weak association with this particular model membrane system.

## DISCUSSION

Our RP-HPLC studies demonstrate that the retention times (and, by inference, the effective hydrophobicities) of the series of peptides of the general structure acetyl-K<sub>2</sub>-(L<sub>m</sub>+A<sub>n</sub>)-K<sub>2</sub>-amide decrease as the Leu/Ala ratio decreases, as expected, given that leucine is more hydrophobic than alanine (35–37). However, these studies also show that the effective hydrophobicities of the three compositionally isomeric peptides, A<sub>7</sub>L<sub>10</sub>A<sub>7</sub>, L<sub>3</sub>A<sub>4</sub>, and LA<sub>2</sub>L<sub>2</sub>A<sub>2</sub> (Leu/Ala ratio of 10/14), also differ appreciably, with effective hydrophobicity increasing in the following order: A<sub>7</sub>L<sub>10</sub>A<sub>7</sub> < L<sub>3</sub>A<sub>4</sub> < LA<sub>2</sub>L<sub>2</sub>A<sub>2</sub>. Clearly, this observation reflects differences in the spatial distribution of Leu and Ala residues on their  $\alpha$ -helical surfaces. With LA<sub>2</sub>L<sub>2</sub>A<sub>2</sub>, the more hydrophobic Leu residues are all linearly clustered on one face of the  $\alpha$ -helix, thereby maximizing the size of the contiguous hydrophobic surface available for interaction with hydrophobic surfaces such as the stationary phase of the RP-HPLC column. In contrast, the Leu residues of L<sub>3</sub>A<sub>4</sub> are more evenly dispersed over the surface of the  $\alpha$ -helix, and as a result, the sizes of all

contiguous hydrophobic patches on its surface are markedly reduced. Finally, with A<sub>7</sub>L<sub>10</sub>A<sub>7</sub>, the Leu residues are cylindrically clustered in the central portion of the nonpolar helical core, and because of the curvature of the helical rod, the size of any contiguous hydrophobic surface which can interact with the RP-HPLC stationary phase is actually smaller than with the other two peptides. The differences between the effective hydrophobicities of these three compositionally isomeric  $\alpha$ -helical peptides can thus be attributed to differences between the relative sizes of contiguous hydrophobic patches on their helical surfaces. The effect of the distribution and localization of Leu and Ala residues in the nonpolar core of compositionally isomeric peptide helices on the interactions of such peptides with lipid bilayers is currently being investigated. However, our results suggest that clustering of hydrophobic amino acid residues on one face of a peptide  $\alpha$ -helix will also enhance the affinity of such a peptide for lipid bilayers. This consideration influenced our decision to focus on peptides LA<sub>3</sub>LA<sub>2</sub> and LA<sub>6</sub> to explore the lower limits of peptide hydrophobicity required to maintain stable transmembrane associations with lipid bilayers.

Our present temperature profiling RP-HPLC, and our previous and current CD and FTIR spectroscopic studies, indicate that in general, the propensity of this series of peptides to form stable helical structures in aqueous solution, in SDS micelles, or in phospholipid bilayers decreases as the Leu/Ala ratio in the central core of the peptide decreases. Moreover, the propensity of this series of peptides to form stable helical structures also increases as the hydrophobicity of the environment of the nonpolar core increases (i.e., in going from water to SDS micelles to PC bilayers). These two results can be rationalized by considering recent studies of the intrinsic helix forming propensities of various aliphatic hydrophobic amino acid residues in water and of the overall stability of peptide helices formed by such amino acids. These studies indicate that whereas the intrinsic helix forming propensity decreases in the order Ala > Leu > Ile > Val, helical stability actually decreases in the order Leu > Ile > Ala > Val (see refs 36 and 37). Given that the hydrophobicities of these peptides decrease in the order Ile ~ Leu > Val > Ala, we have suggested that the stability of peptide helices in aqueous media is actually a reflection of both the intrinsic helix forming propensity of their amino acid residues and the hydrophobicities of the amino acid side chains (see refs 34 and 35). However, other studies suggest that the  $\alpha$ -helical propensities of the same hydrophobic amino acids decrease in the order Ile > Leu > Val > Ala (37–40). The results of these various studies can be reconciled if one assumes the latter studies were actually measuring helical stability and not intrinsic helix forming propensity per se. Nevertheless, the results of our structural studies of this series of peptides are generally in accord with the results of both sets of studies. Moreover, both sets of studies agree that the intrinsic  $\alpha$ -helix forming propensities of the various amino acids are higher in nonpolar solvents such as butanol (dielectric constant of ~17.8 units at 25 °C) than in water. Thus, in the less polar environment of the hydrophobic core of SDS micelles and especially in phospholipid bilayers, the  $\alpha$ -helix forming propensities of these aliphatic amino acid residues should be greater than observed in water or butanol, and the differences between the  $\alpha$ -helix forming propensities of the

individual residues should also be greater. Our observations of the relative  $\alpha$ -helical propensities of these peptides in different environments reported in this and previous work (4, 14, 19, 23) are compatible with these general principles. Interestingly, the ranking order Ile > Leu > Val > Ala is also the order of the decreasing abundance of these aliphatic amino acid residues in the  $\alpha$ -helical transmembrane segments of monotopic membrane proteins (41, 42). This suggests that these amino acids may have been selected for enrichment in the transmembrane segments of integral membrane proteins at least in part on the basis of their  $\alpha$ -helix forming propensities in the nonpolar environment of the membrane interior, as well as for their hydrophobic natures (23).

Our transmission FTIR results indicate that LA<sub>3</sub>LA<sub>2</sub> and LA<sub>6</sub> are both predominantly associated with PC bilayers, since their conformation is reversibly altered when the host phospholipid bilayer membrane lipid undergoes its gel-liquid-crystalline phase transition and that this temperature-induced conformational change is more pronounced with the former than the latter peptide. Moreover, LA<sub>3</sub>LA<sub>2</sub> undergoes much less extensive H-D amide exchange when incorporated into PC bilayers than does LA<sub>6</sub>, suggesting that the latter peptide may be undergoing more extensive exchange between the aqueous and membrane environments. Alternatively or in addition, LA<sub>6</sub> may not be localized in the host phospholipid bilayer exclusively in a transmembrane orientation but may instead reside in the glycerol backbone region of the PC bilayer in an orientation parallel to the membrane plane (see below). These suggestions are supported by the DSC results presented here, which indicate that LA<sub>3</sub>LA<sub>2</sub> and especially LA<sub>6</sub> have markedly weaker effects on the thermotropic phase behavior of the host PC bilayer than do the more hydrophobic peptides L<sub>24</sub> and (LA)<sub>12</sub>, but a larger effect than does the incorporation of the less hydrophobic peptide A<sub>24</sub>, which has an only very slight effect (23). Considering that the FTIR experiments were carried out in very concentrated aqueous peptide/lipid dispersions whereas the DSC experiments were performed with much more dilute peptide/lipid vesicles, the apparently stronger association of these peptides with phospholipid bilayers in the former as compared to the latter experiments is understandable, given the markedly different volumes of the aqueous phases in these two types of experiments.

We have shown previously that L<sub>24</sub> (5, 14) and (LA)<sub>12</sub> (19) remain strongly associated with the unhydrated or hydrated phospholipid bilayers into which these peptides were initially incorporated and that these two peptides exist essentially entirely as transbilayer  $\alpha$ -helices in phospholipid model membranes. In contrast, A<sub>24</sub> also remains strongly associated as a transmembrane  $\alpha$ -helix in the unhydrated phospholipid bilayers into which they were initially incorporated, but in fully hydrated phospholipid bilayers, this peptide exists as a mixture of helical and random coil structures which partition strongly into the aqueous phase, when present (23). For this study, peptides LA<sub>3</sub>LA<sub>2</sub> and LA<sub>6</sub> were designed such that the most hydrophobic residues would be linearly clustered on one face of the  $\alpha$ -helix, a topology expected to maximize the propensity for interaction with hydrophobic surfaces (see RP-HPLC data). Nevertheless, they still exhibit an intermediate behavior in which they exist as  $\alpha$ -helices in unhydrated PC bilayers and as a mixture 3<sub>10</sub>- and  $\alpha$ -helical structures in hydrated PC bilayers. Also, they

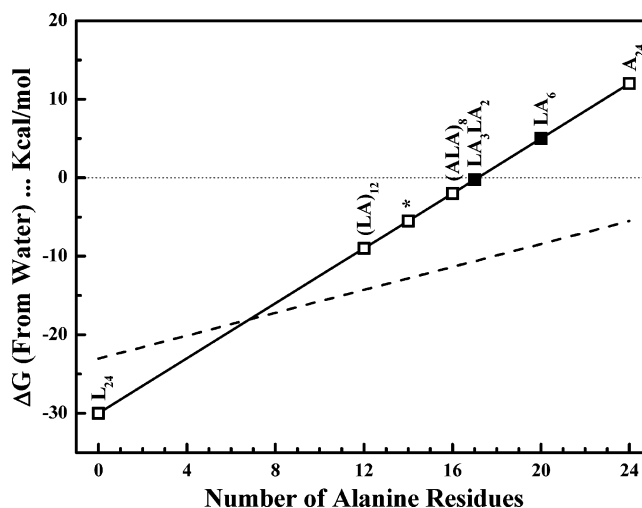


FIGURE 12: Calculated water-bilayer partitioning free energies of the acetyl-K<sub>2</sub>-(L<sub>m</sub>-A<sub>n</sub>)-K<sub>2</sub>-amide family of model transmembrane  $\alpha$ -helical peptides. The calculations were based on the whole-residue water-octanol partitioning free energy scale developed by White and co-workers (40, 41). These calculations were restricted to the hydrophobic core of the peptides and assumed that the peptides were completely  $\alpha$ -helical. The data for peptides highlighted in this study are depicted with filled symbols, and the asterisk marks the data point calculated for the compositional isomers with hydrophobic cores composed of 10 Leu and 14 Ala residues. For comparative purposes, comparable calculations using the whole-residue water-membrane interface partitioning free energies are depicted with the dashed line.

are mostly associated with phospholipid model membranes in concentrated peptide/lipid dispersions but more associated with the aqueous phase in dilute solutions. These results suggest that despite the advantages conferred by linear clustering of the most hydrophobic residues, LA<sub>3</sub>LA<sub>2</sub> and especially LA<sub>6</sub> may not be sufficiently hydrophobic to be associated exclusively with lipid bilayers in the biologically relevant situation, where water is normally present in great excess.

Our experimental data can also be rationalized on the basis of the relative overall hydrophobicities of the peptides as exemplified by the experimentally determined hydrophobicity scales derived from the partitioning of the amino acid residues of short unstructured peptides into membrane polar-apolar interfaces and into octanol (see refs 28 and 29). On the basis of these hydrophobicity scales, Leu residues are expected to strongly prefer the lipid bilayer interface and especially the lipid bilayer hydrophobic core over water, whereas Ala residues should exhibit a slight preference for water over the phospholipid bilayer polar-apolar interface and a fairly strong preference for water over the hydrophobic interior of the phospholipid bilayer. Indeed, using these hydrophobicity scales, the free energies for the transfer of the nonpolar central regions of peptides L<sub>24</sub>, (LA)<sub>12</sub>, LA<sub>3</sub>-LA<sub>2</sub>, LA<sub>6</sub>, and A<sub>24</sub> (as  $\alpha$ -helices) from water to the hydrophobic cores of phospholipid bilayers, modeled by partitioning into *n*-octanol, were estimated to be -30.0, -9.0, -0.3, 5.0, and 12.0 kcal/mol, respectively, and values of -23.0, -14.3, -10.6, -8.4, and -5.5 kcal/mol, respectively, were estimated for their transfer from water to the bilayer polar-apolar interfaces (see Figure 12). It is also interesting to note that if the two dilysine caps of these peptides are included in these calculations, free energy estimates for transferring these peptides (as  $\alpha$ -helices) from water to the

hydrophobic core of a phospholipid bilayer were  $-16.1$ ,  $-4.9$ ,  $5.2$ ,  $18.9$ , and  $25.9$  kcal/mol, respectively, and  $-23.2$ ,  $-14.5$ ,  $-10.8$ ,  $-8.6$ , and  $-5.7$  kcal/mol, respectively, for their transfer from water to the bilayer polar–apolar interfacial region (Figure 12). Given these free energy estimates,  $LA_6$ , like  $A_{24}$ , would not be expected to partition into the hydrophobic domains of lipid bilayers in a transmembrane orientation, whereas  $LA_3LA_2$  would have an approximately near-equal probability of partitioning into water or into the hydrophobic core of phospholipid bilayers in a transbilayer topology. Interestingly, the water–membrane partitioning free energies calculated for this family of Leu-Ala copolymers also suggest that members with hydrophobic cores containing eight or more Ala residues [e.g.,  $(LA)_{12}$ ] should partition into the membrane polar–apolar interfacial region in preference to the hydrophobic core of the bilayer (see Figure 12, dashed line). However, studies performed by us (19) and others (43–45) have shown that polar capped peptides with hydrophobic cores comparable to that of  $(LA)_{12}$  partition preferentially into the hydrophobic regions of phospholipid bilayers in a transmembrane orientation. Thus, it appears that partitioning free energies calculated on the basis of water–octanol partitioning are probably better predictors of the behavior of this family of model transmembrane  $\alpha$ -helical peptides than are those based on water–membrane interface partitioning.

Recent studies of alanine-rich peptides containing varying numbers of leucine residues by Lafleur and co-workers have shown that there are both minimal length and minimal hydrophobicity requirements for the spontaneous insertion of such peptides into preformed phospholipid vesicles (43). Interestingly, however, these workers also showed that for peptides which meet these criteria, the presence of lysine caps at both ends of the peptide prevents spontaneous insertion into preformed phospholipid vesicles, despite the fact that such peptides remain associated with lipid bilayers if first cosolubilized with phospholipid prior to vesicle formation. It was therefore concluded that the translocation of two of the charged lysine residues through the hydrophobic core of the preformed lipid vesicles represents a significant energy barrier against their spontaneous insertion into preformed lipid bilayers. In our studies, peptide lipid mixtures were all prepared by cosolubilization in organic solvent prior to the formation of the lipid vesicles, and these peptides are shown to be helical and in a transbilayer orientation prior to addition of water. However, it is apparent that translocation of the dilysine termini of  $A_{24}$  and  $LA_6$  through the hydrophobic regions of the hydrophobic core of the lipid bilayer occurs quite readily upon hydration. Apparently, the free energy of partitioning of  $A_{24}$  and  $LA_6$  into water is large enough to overcome this energy barrier, whereas the behavior of  $LA_3LA_2$  in this regard is marginal.

It is interesting to compare our in vitro results with the results of studies of the nature and length of the hydrophobic helices in natural proteins required for stop transfer in the translocon and stable insertion into the lipid bilayer of the host biological membrane (see refs 46–48 and references cited therein). For the stop transfer reaction, the specific number of amino acids required depends on the hydrophobicity of the potential transmembrane sequence. For example, it appears that at least 20 Ala residues, but only  $\sim 9$ –10 Leu residues, are required for near-complete stop transfer,

although the presence of polar amino acids within this sequence and positively charged amino acid residues after this sequence can also play a role. More directly relevant to this study, however, are the nature and length of the transmembrane segment required for a stable transmembrane insertion in the lipid bilayer, once the potential transmembrane sequence is released from the translocon. Kuroiwa et al. (46) reported that when a 21-amino acid sequence of hydrophobic amino acids was inserted into interleukin 2, a typical secretory protein, this sequence caused interleukin to become membrane-associated if it contained only Leu residues or roughly equal numbers of Leu and Ala residues, but not if it contained only a single Leu residue. Chen and Kendall (47) subsequently reported that 21-residue transmembrane segments inserted into *Escherichia coli* alkaline phosphatase, a transported, water-soluble protein, partitioned into the membrane fraction (84 and 94%, respectively) if it contained 10 or 20 Leu residues but not if it contained only Ala residues (only 2% membrane association). Finally, Hessa et al. (48) recently calculated that in an engineered peptide with a 19-residue hydrophobic stretch, containing only Leu and Ala residues, at least four Leu residues were required to make the free energy of partitioning of the peptide into a lipid bilayer favorable and at least six Leu residues to raise the probability of bilayer insertion above 0.9. When one considers that the length of the hydrophobic sequences of the peptides studied here is 24 amino acids, our finding that more than seven Leu residues are required for stable transmembrane association agrees fairly well with these previous in vitro protein cotranslational studies.

In conclusion, we note that  $A_{24}$  and  $LA_6$  clearly do not form a stable transmembrane association with fully hydrated phospholipid bilayers. Although it is feasible to insert these peptides into dry phospholipid films as a transmembrane helix, this association is not maintained upon hydration of these films, presumably because these peptides preferentially partition into the aqueous phase. Preferential partitioning of  $A_{24}$  and  $LA_6$  into the aqueous phase is undoubtedly the combined result of their appreciable solubility in aqueous media and the fact that the volume of the aqueous compartment greatly exceeds that of the lipid phase. Our findings can therefore be attributed to the fact that the helical surfaces of  $A_{24}$  and  $LA_6$  are not sufficiently hydrophobic for these peptides to form a stable association with the hydrophobic core of the lipid bilayer, either as dispersed monotopic helices or as peptide aggregates. Moreover, even the more hydrophobic peptide  $LA_3LA_2$  may not form a sufficiently stable association with phospholipid bilayers to exist exclusively in a permanent transmembrane orientation in the presence of a large excess of water, suggesting that its hydrophobicity is at best marginal in this regard. These observations also indicate that highly alanine-rich peptides are actually poor models of the helical transmembrane segments of membrane proteins and poor candidates for spontaneous insertion into preformed lipid bilayers. These latter conclusions are compatible with the results of a number of other experimental observations (49, 50) and with the finding that alanine is the least abundant of the aliphatic amino acids present in the transmembrane segments of monotopic membrane proteins (41, 42). We therefore suggest that both  $\alpha$ -helical propensity and hydrophobicity are important parameters in determining the suitability of aliphatic amino acid residues



in forming stable transmembrane  $\alpha$ -helices in a lipid bilayer environment.

## REFERENCES

- Lewis, R. N. A. H., Zhang, Y. P., Liu, F., and McElhaney, R. N. (2002) Mechanisms of the interaction of  $\alpha$ -helical transmembrane peptides with phospholipid bilayers, *Bioelectrochemistry* 56, 135–140.
- de Planque, M. R. R., and Killian, J. A. (2003) Protein-lipid interactions studied with designed transmembrane peptides: Role of hydrophobic matching and interfacial anchoring, *Mol. Membr. Biol.* 20, 271–284.
- Davis, J. H., Clare, D. M., Hodges, R. S., and Bloom, M. (1983) Interaction of a synthetic amphiphilic polypeptide and lipids in a bilayer structure, *Biochemistry* 22, 5298–5305.
- Zhang, Y. P., Lewis, R. N. A. H., Hodges, R. S., and McElhaney, R. N. (1992) FTIR spectroscopic studies of the conformation and amide hydrogen exchange of a peptide model of the hydrophobic transmembrane  $\alpha$ -helices of membrane proteins, *Biochemistry* 31, 11572–11578.
- Zhang, Y. P., Lewis, R. N. A. H., Hodges, R. S., and McElhaney, R. N. (1992) Interaction of a peptide model of a hydrophobic transmembrane  $\alpha$ -helical segment of a membrane protein with phosphatidylcholine bilayers: Differential scanning calorimetric and FTIR spectroscopic studies, *Biochemistry* 31, 11579–11588.
- Axelsen, P. H., Kaufman, P. H., McElhaney, R. N., and Lewis, R. N. A. H. (1995) The infrared dichroism of transmembrane helical polypeptides, *Biophys. J.* 69, 2770–2781.
- Huschilt, J. C., Millman, B. M., and Davis, J. H. (1989) Orientation of  $\alpha$ -helical peptides in a lipid bilayer, *Biochim. Biophys. Acta* 979, 139–141.
- Bolen, E. J., and Holloway, P. W. (1990) Quenching of tryptophan fluorescence by brominated phospholipid, *Biochemistry* 29, 9638–9643.
- Huschilt, J. C., Hodges, R. S., and Davis, J. H. (1985) Phase equilibria in an amphiphilic peptide-phospholipid model membrane by deuterium nuclear magnetic resonance difference spectroscopy, *Biochemistry* 24, 1377–1386.
- Morrow, M. R., Huschilt, J. C., and Davis, J. H. (1985) Simultaneous modeling of phase and calorimetric behavior in an amphiphilic peptide/phospholipid model membrane, *Biochemistry* 24, 5396–5406.
- Zhang, Y.-P., Lewis, R. N. A. H., Hodges, R. S., and McElhaney, R. N. (1995) Interaction of a peptide model of a hydrophobic transmembrane  $\alpha$ -helical segment of a membrane protein with phosphatidylethanolamine bilayers: Differential scanning calorimetric and FTIR spectroscopic studies, *Biophys. J.* 68, 847–857.
- Pauls, K. P., MacKay, A. L., Soderman, O., Bloom, M., Taneja, A. K., and Hodges, R. S. (1985) Dynamic properties of the backbone of an integral membrane polypeptide measured by  $^2\text{H}$  NMR, *Eur. Biophys. J.* 12, 1–11.
- Subczynski, W. K., Lewis, R. N. A. H., McElhaney, R. N., Hodges, R. S., Hyde, J. S., and Kusumi, A. (1998) Molecular organization and dynamics of 1-palmitoyl-2-oleoyl-phosphatidylcholine bilayers containing a transmembrane  $\alpha$ -helical peptide, *Biochemistry* 37, 3156–3164.
- Liu, F., Lewis, R. N. A. H., Hodges, R. S., and McElhaney, R. N. (2002) Effect of variations in the structure of a poly-leucine-based  $\alpha$ -helical transmembrane peptide on its interaction with phosphatidylcholine bilayers, *Biochemistry* 41, 9197–9207.
- Liu, F., Lewis, R. N. A. H., Hodges, R. S., and McElhaney, R. N. (2004) Effect of variations in the structure of a poly-leucine-based  $\alpha$ -helical transmembrane peptide on its interactions with phosphatidylethanolamine bilayers, *Biophys. J.* 87, 2470–2482.
- Liu, F., Lewis, R. N. A. H., Hodges, R. S., and McElhaney, R. N. (2004) Effect of variations in the structure of a poly-leucine-based  $\alpha$ -helical transmembrane peptide on its interactions with phosphatidylglycerol bilayers, *Biochemistry* 43, 3679–3687.
- Liu, F., Lewis, R. N. A. H., Hodges, R. S., and McElhaney, R. N. (2001) A differential scanning calorimetric and  $^{31}\text{P}$  NMR spectroscopic study of the effect of transmembrane  $\alpha$ -helical peptides on the lamellar/reversed hexagonal phase transition of phosphatidylethanolamine model membranes, *Biochemistry* 40, 760–768.
- Zhang, Y. P., Lewis, R. N. A. H., Henry, G. D., Sykes, B. D., Hodges, R. S., and McElhaney, R. N. (1995) Peptide models of helical hydrophobic transmembrane segments of membrane proteins. I. Studies of the conformation, intrabilayer orientation and amide hydrogen exchangeability of Ac-K<sub>2</sub>-(LA)<sub>12</sub>-K<sub>2</sub>-amide, *Biochemistry* 34, 2348–2361.
- Zhang, Y. P., Lewis, R. N. A. H., Henry, G. D., Hodges, R. S., and McElhaney, R. N. (1995) Peptide models of helical hydrophobic transmembrane segments of membrane proteins. II. DSC and FTIR spectroscopic studies of the interaction of Ac-K<sub>2</sub>-(LA)<sub>12</sub>-K<sub>2</sub>-amide with phosphatidylcholine bilayers, *Biochemistry* 34, 2362–2371.
- Pare, C., Lafleur, M., Liu, F., Lewis, R. N. A. H., and McElhaney, R. N. (2001) Differential scanning calorimetry and  $^2\text{H}$ -nuclear magnetic resonance and Fourier transform infrared spectroscopic studies of the effects of transmembrane  $\alpha$ -helical peptides on the organization of phosphatidylcholine bilayers, *Biochim. Biophys. Acta* 1511, 60–73.
- Zhang, Y. P., Lewis, R. N. A. H., Hodges, R. S., and McElhaney, R. N. (2001) Peptide models of the helical hydrophobic transmembrane segments of membrane proteins: Interactions of acetyl-K<sub>2</sub>-(LA)<sub>12</sub>-K<sub>2</sub>-amide with phosphatidylethanolamine bilayer membranes, *Biochemistry* 40, 474–482.
- Subczynski, W. K., Pasenkiewicz-Gierula, M., McElhaney, R. N., Hyde, J. S., and Kusumi, A. (2003) Molecular dynamics of 1-palmitoyl-2-oleoylphosphatidylcholine membranes containing transmembrane  $\alpha$ -helical peptides with alternating leucine and alanine residues, *Biochemistry* 42, 3939–3948.
- Lewis, R. N. A. H., Zhang, Y. P., Hodges, R. S., Subczynski, W. K., Kusumi, A., Flach, C. R., Mendelsohn, R., and McElhaney, R. N. (2001) A polyalanine-based peptide cannot form a stable transmembrane  $\alpha$ -helix in fully hydrated phospholipid bilayers, *Biochemistry* 40, 12103–12111.
- Liu, P. Z., and Baldwin, R. L. (1997) Mechanism of helix induction by trifluoroethanol: A framework for extrapolating the helix-forming properties of peptides from trifluoroethanol/water mixtures back to water, *Biochemistry* 36, 8413–8421.
- Lee, D. J., Mant, C. T., and Hodges, R. S. (2003) A novel method to measure self-association of small amphipathic molecules: Temperature profiling in reversed-phase chromatography, *J. Biol. Chem.* 278, 22918–22927.
- Mant, C. T., Chen, Y., and Hodges, R. S. (2003) Temperature profiling of polypeptides in reversed-phase liquid chromatography. I. Monitoring of dimerization of amphipathic  $\alpha$ -helical peptides, *J. Chromatogr., A* 1009, 29–43.
- Mant, C. T., Tripet, B., and Hodges, R. S. (2003) Temperature profiling of polypeptides in reversed-phase liquid chromatography. II. Monitoring of folding and stability of two-stranded  $\alpha$ -helical coiled-coils, *J. Chromatogr., A* 1009, 45–59.
- Wimley, W. C., and White, S. H. (1996) Experimentally determined hydrophobicity scale for proteins at membrane interfaces, *Nat. Struct. Biol.* 3, 842–848.
- White, S. H., and Wimley, W. C. (1999) Membrane protein folding and stability: Physical principles, *Annu. Rev. Biophys. Biomol. Struct.* 28, 319–365.
- Mantsch, H. H., Madec, C., Lewis, R. N. A. H., and McElhaney, R. N. (1985) The thermotropic phase behavior of model membranes composed of phosphatidylcholines containing isobranched fatty acids. II. Infrared and  $^{31}\text{P}$ -NMR spectroscopic studies, *Biochemistry* 24, 2440–2446.
- Tamm, L. K., and Tatulian, S. A. (1997) Infrared spectroscopy of proteins and peptides in lipid bilayers, *Q. Rev. Biophys.* 30, 365–429.
- Chirgadze, Y. N., and Brazhnikov, E. V. (1974) Intensities and other spectral parameters of infrared amide bands of polypeptides in  $\alpha$ -helical form, *Biopolymers* 13, 1701–1712.
- Lewis, R. N. A. H., and McElhaney, R. N. (1998) The structure and organization of phospholipid bilayers as revealed by infrared spectroscopy, *Chem. Phys. Lipids* 96, 9–21.
- Lewis, R. N. A. H., and McElhaney, R. N. (2002) Vibrational Spectroscopy of lipids, in *Handbook of Vibrational Spectroscopy* (Chalmers, J. M., and Griffith, P. R., Eds.) Vol. 5, pp 3447–3464, John Wiley and Sons, Chichester, England.
- Zhou, N. E., Monera, O. D., Kay, C. M., and Hodges, R. S. (1994)  $\alpha$ -Helical propensities of amino acids in the hydrophobic face of an amphipathic  $\alpha$ -helix, *Protein Pept. Lett.* 1, 114–119.
- Monera, O. D., Serada, T. J., Zhou, N. E., Kay, C. M., and Hodges, R. S. (1995) Relationship of sidechain hydrophobicity and  $\alpha$ -helical propensity on the stability of the single-stranded amphipathic  $\alpha$ -helix, *J. Pept. Sci.* 1, 319–329.

37. Lis, S.-C., and Deber, C. M. (1994) A measure of helical propensity for amino acids in membrane environments, *Nat. Struct. Biol.* *1*, 368–373.
38. Deber, C. M., and Li, S.-C. (1995) Peptides in membranes  $\alpha$ -helicity and hydrophobicity, *Biopolymers* *37*, 295–318.
39. Liu, L.-P., and Deber, C. M. (1998) Uncoupling hydrophobicity and helicity in transmembrane segments:  $\alpha$ -Helical propensities of the amino acids in non-polar environments, *J. Biol. Chem.* *273*, 23645–23648.
40. Blondelle, S. E., Forood, B., Houghten, R. A., and Perez-Paya, E. (1997) Secondary structure induction in aqueous vs. membrane-like environments, *Biopolymers* *42*, 489–498.
41. Jones, D. T., Taylor, W. R., and Thornton, J. M. (1994) A model approach to the prediction of all-helical membrane protein structure and topology, *Biochemistry* *33*, 3038–3049.
42. Landolt-Marticorena, C., Williams, K. A., Deber, C. M., and Reithmeier, R. A. F. (1993) Nonrandom distribution of amino acid in the transmembrane segments of human type-I single span membrane proteins, *J. Mol. Biol.* *229*, 602–608.
43. Percot, H., Zhu, X. X., and Lafleur, M. (1999) Design and characterization of anchoring amphiphilic peptides and their interactions with lipid vesicles, *Biopolymers* *50*, 647–655.
44. Killian, J. A. (1998) Hydrophobic mismatch between proteins and lipids in membranes, *Biochim. Biophys. Acta* *1376*, 401–416.
45. de Planque, M. R. R., and Kilian, J. A. (2003) Protein-lipid interactions studied with designed transmembrane peptides: Role of hydrophobic matching and interfacial anchoring, *Mol. Membr. Biol.* *20*, 271–284.
46. Kuriowa, T., Sakaguchi, M., Mihara, K., and Omura, T. (1991) Systematic analysis of stop-transfer sequence for microsomal membrane, *J. Biol. Chem.* *266*, 9251–9255.
47. Chen, H., and Kendall, D. A. (1995) Artificial transmembrane segments. Requirement for stop transfer and polypeptide orientation, *J. Biol. Chem.* *270*, 14115–14122.
48. Hessa, T., Kim, H., Bihlmaier, K., Lundin, C., Boekel, J., Andersson, H., Nilsson, I., White, S. H., and von Heijne, G. (2005) Recognition of transmembrane helices by the endoplasmic reticulum translocon, *Nature* *433*, 377–381.
49. Moll, T. S., and Thompson, T. E. (1994) Semisynthetic proteins: Model systems for the study of the insertion of hydrophobic peptides into preformed lipid bilayers, *Biochemistry* *33*, 15469–15482.
50. Chung, L. A., and Thompson, T. E. (1996) Design of membrane-inserting peptides: Spectroscopic characterization with and without lipid bilayers, *Biochemistry* *35*, 11343–11354.

BI061891B